

PACS numbers: 42.65.Ky; 42.70.Nq
DOI: 10.1070/QE2007v037n01ABEH013266

Spectral distribution of the efficiency of terahertz difference frequency generation upon collinear propagation of interacting waves in semiconductor crystals

S.N. Orlov, Yu.N. Polivanov

Abstract. **Dispersion phase matching curves and spectral distributions of the efficiency of difference frequency generation in the terahertz range are calculated for collinear propagation of interacting waves in zinc blende semiconductor crystals (ZnTe, CdTe, GaP, GaAs). The effect of the pump wavelength, the nonlinear crystal length and absorption in the terahertz range on the spectral distribution of the efficiency of difference frequency generation is analysed.**

Keywords: *difference frequency generation, terahertz radiation, dispersion phase matching, polaritons.*

1. Introduction

Studies devoted to the development of tunable radiation sources in the terahertz spectral range based on nonlinear optical excitation of photon polaritons of the lower dispersion branch in non-centre symmetric crystals have become recently very active (a review of earlier papers in this field is presented in [1]). This is explained by new potential possibilities of using such radiation in many problems of three-dimensional tomography, chemistry, and biology (including the diagnostics of cancer), for detecting explosives, etc. (see, for example, [2]). Note that at present, along with traditional schemes of nonlinear optical generation of terahertz radiation, which use, as a rule, narrowband lasers for excitation [1 – 7], various process of excitation by femtosecond pulses, whose spectral width exceeds the terahertz radiation frequency, are being actively studied (see, for example, [2, 8 – 12].

It is known that the phase matching condition, which is required for efficient nonlinear optical excitation of polaritons of the lower dispersion branch in the field of two pump waves (biharmonic pumping), can be fulfilled not only in optically anisotropic but in optically isotropic crystals both upon noncollinear and collinear propagation of interacting waves. In the latter case, the phase matching condition can be changed by tuning the biharmonic pump frequencies (dispersion phase matching [13, 14]). In this connection the nonlinear optical generation of terahertz radiation was also studied in optically isotropic non-centre symmetric semiconductor crystals, which often have higher quadratic nonlinear susceptibilities compared to those for dielectric crystals. In this case, however, the spectral distribution of the efficiency of difference frequency generation in the low-frequency spectral region during collinear propagation of interacting waves in optically isotropic crystals considerably differs from the distribution in the case of phase matching realised due to noncollinearity or changing the propagation direction of waves in anisotropic crystals.

In this paper, we analyse the spectral distribution of the efficiency of difference frequency generation in the terahertz range during collinear propagation of interacting waves for some specific zinc blende cubic non-centre symmetric two-atom semiconductor crystals of practical interest belonging to the point symmetry group $\bar{4}3m$ and having one triply degenerate optical lattice vibration. The simplicity of the crystal structure allows us to calculate the spectral distribution by taking explicitly into account the dispersion of polaritons and dispersion of the quadratic nonlinear susceptibility in the region of the lattice resonance of these crystals.

2. Dispersion phase matching

Phase matching for the three-wave parametric mixing process under study ($\omega = \omega_p - \omega_s$) is determined from the condition

$$\boldsymbol{k}_p(\omega_p) - \boldsymbol{k}_s(\omega_s) = \boldsymbol{k}'(\omega). \quad (1)$$

Here, ω_p, ω_s, ω, $\boldsymbol{k}_p$, $\boldsymbol{k}_s$, and $\boldsymbol{k}'$ are the frequencies and wave vectors of the high- and low-frequency pumping, and terahertz radiation, respectively. For convenience of the analysis of phase matching conditions, we will use the polariton representation of terahertz radiation waves, by assuming that they are polaritons of the lower dispersion branch and are excited by laser radiation at frequencies ω_p and ω_s located in the transparency region of a crystal. Because polaritons of the lower dispersion branch are noticeably absorbed, the wave vector of polaritons $\boldsymbol{k}$ is the complex quantity, i.e. $k(\omega) = k'(\omega) + ik''(\omega)$.

The dispersion of polaritons in the single-phonon resonance approximation can be represented in the form

$$\frac{k^2c^2}{\omega^2} = \varepsilon(\omega) = \varepsilon_\infty + \frac{(\varepsilon_0 - \varepsilon_\infty)\omega_0^2}{\omega_0^2 - \omega^2 - i\omega\Gamma}. \quad (2)$$

S.N. Orlov, Yu.N. Polivanov A.M. Prokhorov General Physics Institute, Russian Academy of Sciences, ul. Vavilova 38, 119991 Moscow, Russia; e-mail: orlov@kapella.gpi.ru, polivano@kapella.gpi.ru

Received 29 May 2006; revision received 13 July 2006
Kvantovaya Elektronika **37** (1) 36 – 42 (2007)
Translated by M.N. Sapozhnikov

Here, ω_0 and Γ are the frequency and decay of transverse optical phonons; $\varepsilon(\omega)$ is the permittivity of the crystal at frequency ω; $\varepsilon_0 = \varepsilon(0) \equiv n^2(0)$; and $\varepsilon_\infty = \varepsilon(\omega \gg \omega_0)$. In the region of weak polariton absorption of interest for us, i.e. for $k'(\omega) \gg \alpha(\omega) \equiv 2k''(\omega)$, we can obtain from (2) the approximate relations

$$k'(\omega) = \frac{\omega}{c} n(\omega) = \frac{\omega}{c} \mathrm{Re}\sqrt{\varepsilon(\omega)} \approx \frac{\omega}{c}\left[\varepsilon_\infty + \frac{(\varepsilon_0 - \varepsilon_\infty)\omega_0^2}{\omega_0^2 - \omega^2}\right]^{1/2}$$

$$= \frac{\omega}{c}\left(\frac{\varepsilon_0\omega_0^2 - \varepsilon_\infty\omega^2}{\omega_0^2 - \omega^2}\right)^{1/2}, \quad (3)$$

$$\alpha(\omega) = 2k''(\omega) = 2\frac{\omega}{c}\mathrm{Im}\sqrt{\varepsilon(\omega)} \approx \frac{\omega}{c}\frac{\mathrm{Im}\,\varepsilon(\omega)}{n(\omega)}$$

$$= \frac{\omega}{cn(\omega)}\frac{(\varepsilon_0 - \varepsilon_\infty)\omega_0^2}{(\omega_0^2 - \omega^2)^2}\omega\Gamma, \quad (4)$$

where $n(\omega)$ and $\alpha(\omega)$ are refractive index and absorption coefficient of a polariton wave at frequency ω.

To make the subsequent analysis illustrative, we introduce the difference wave vector $\boldsymbol{q}(\omega_\mathrm{p}, \omega) = \boldsymbol{k}_\mathrm{p}(\omega_\mathrm{p}) - \boldsymbol{k}_\mathrm{s}(\omega_\mathrm{p} - \omega)$. The modulus of this vector in the case of collinear interaction, taking into account only the linear term in the expansion of k_s in $\omega \ll \omega_\mathrm{p}$, can be written in the form

$$q(\omega_\mathrm{p}, \omega) \equiv k_\mathrm{p}(\omega_\mathrm{p}) - k_\mathrm{s}(\omega_\mathrm{p} - \omega)$$

$$= \frac{\omega_\mathrm{p} n(\omega_\mathrm{p}) - (\omega_\mathrm{p} - \omega)n(\omega_\mathrm{p} - \omega)}{c}$$

$$\approx \frac{\omega}{c}\left[n(\omega_\mathrm{p}) + \omega_\mathrm{p}\frac{\partial n}{\partial\omega}\bigg|_{\omega_\mathrm{p}}\right] = \frac{\omega}{V_\mathrm{g}(\omega_\mathrm{p})} \equiv \frac{\omega}{c} n_\mathrm{g}(\omega_\mathrm{p}), \quad (5)$$

where

$$n_\mathrm{g}(\omega_\mathrm{p}) = n(\omega_\mathrm{p}) + \omega_\mathrm{p}\frac{\partial n}{\partial\omega}\bigg|_{\omega_\mathrm{p}}$$

is the effective refractive index determining the group velocity $V_\mathrm{g}(\omega_\mathrm{p}) = c/n_\mathrm{g}(\omega_\mathrm{p})$ of the wave at the pump radiation frequency ω_p. Expression (5) is valid for a weak dispersion of the medium in the region of pump frequencies.

The phase matching condition in this approximation takes the form

$$\frac{\omega}{V_\mathrm{g}(\omega_\mathrm{p})} = k(\omega), \quad (6)$$

or

$$V_\mathrm{g}(\omega_\mathrm{p}) = \frac{c}{n(\omega)}, \quad \text{i.e.} \quad n_\mathrm{g}(\omega_\mathrm{p}) = n(\omega),$$

which means that the group velocity $V_\mathrm{g}(\omega_\mathrm{p})$ at the pump wave frequency and the phase velocity $c/n(\omega)$ of polaritons are equal. Note that similar relations were used earlier to analyse the Raman scattering of light by polaritons and calculate phase matching conditions for generation of difference frequency radiation in the IR region (see, for example, [13, 14]).

The graphical determination of frequencies satisfying the phase matching condition is quite illustrative. Figure 1 shows the typical dispersion curve $k(\omega)$ for polaritons of the lower branch and dependences $q(\lambda_\mathrm{p}, \omega) = \omega/V_\mathrm{g}(\omega_\mathrm{p})$ for three different pump wavelengths $\lambda_\mathrm{p} = 2\pi c/\omega_\mathrm{p}$. The intersection points of the dashed straight lines with the dispersion curve determine the polariton frequencies for which the phase matching condition is fulfilled for the given pump wavelength in the case of collinearly propagating interacting waves.

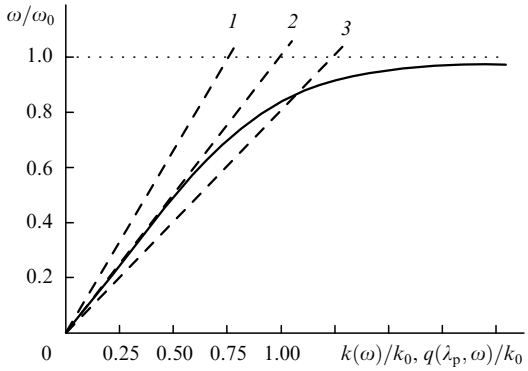

Figure 1. Typical dispersion curve for the lower branch polaritons $k(\omega)$ (solid curve) and functions $q(\lambda_\mathrm{p}, \omega)$ (dashed straight lines) corresponding to pump wavelengths $\lambda_\mathrm{p} > \lambda_\mathrm{cr}$ (*1*), $\lambda_\mathrm{p} = \lambda_\mathrm{cr}$ (*2*), and $\lambda_\mathrm{p} < \lambda_\mathrm{cr}$ (*3*) ($k_0 = \omega_0\sqrt{\varepsilon_\infty}/c$).

Straight line (*2*) in Fig. 1 coincides with the asymptote of the dispersion curve $k(\omega)$ for $\omega \to 0$. The coincidence occurs for a critical pump wavelength $\lambda_\mathrm{p} = \lambda_\mathrm{cr}$ determined by the condition $V_\mathrm{g}(\lambda_\mathrm{cr}) = c/n(0)$, or

$$n_\mathrm{g}(\lambda_\mathrm{cr}) = n(0) \equiv \sqrt{\varepsilon_0}. \quad (7)$$

If the pump wavelength lies in the visible or near-IR region, this condition can be fulfilled only in semiconductor crystals, which have, unlike dielectrics, a considerable dispersion of the refractive index in this region. Straight line (*1*) corresponds to the pump wavelength $\lambda_\mathrm{p} > \lambda_\mathrm{cr}$ for which the phase matching condition is fulfilled only for $\omega = 0$. Note that for $\lambda_\mathrm{p} \geqslant \lambda_\mathrm{cr}$, i.e. for $n_\mathrm{g}(\lambda_\mathrm{p}) \leqslant n(0)$, the lower polariton branch can be completely observed in Raman spectra at small angles [13]; therefore, the phase matching condition for excitation of polaritons by generating difference frequencies can be realised only upon noncollinear propagation of the interacting waves. In this case, a small change in the angle between exciting beams results in a considerable change in the direction of the wave vector of terahertz radiation because k_p, $k_\mathrm{s} \gg k$, which can present problems in coupling terahertz radiation out of the crystal [3].

For $\lambda_\mathrm{p} < \lambda_\mathrm{cr}$, the phase matching condition is satisfied simultaneously both for $\omega = 0$ and $\omega \neq 0$ [straight line (*3*) in Fig. 1]. This complicates the spectral distribution of the efficiency of difference frequency radiation compared to distributions in the case of phase matching obtained in the noncollinear scheme or by changing the propagation direction of the interacting waves in anisotropic crystals, when the phase matching condition is fulfilled only for $\omega \neq 0$.

One can see from (6) that the frequency of polaritons for which the phase matching condition is fulfilled depends on the pump wavelength (this dependence was called the dispersion phase matching in [14]). Figure 2 presents the dispersion phase matching curves that we calculated for crystals under study by expressions (1) and (2) [not restricting ourselves to the linear expansion (5)]. The parameters of crystals required for the calculation of polariton dispersion are given in Table 1. The frequencies of longitudinal optical phonons ω_L are related to parameters entering (2) by the expression $\omega_L^2/\omega_0^2 = \varepsilon_0/\varepsilon_\infty$. The values of the refractive index in the optical range were taken from [19].

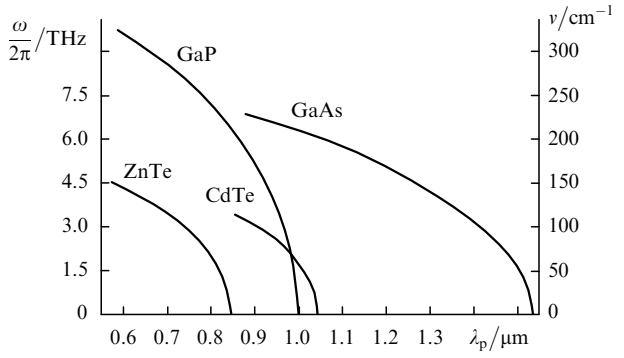

Figure 2. Dispersion phase matching curves upon difference frequency generation in the terahertz range, calculated for different crystals for collinearly propagating interacting waves.

3. Spectral distribution of the efficiency of difference frequency generation

The efficiency $\eta(\omega)$ of radiation generation at the difference frequency $\omega = \omega_p - \omega_s$ in the field of two monochromatic pump waves in the plane wave approximation by neglecting the pump depletion can be described by the expression [20]

$$\eta(\omega) \equiv \frac{P_{THz}}{P_s} = \frac{2\omega^2}{\varepsilon_{vac} c^3} \frac{|d(\omega)|^2}{n(\omega_p) n(\omega_s) n(\omega)} I_p$$

$$\times \frac{\exp[-\alpha(\omega)L] - 2\exp[-\alpha(\omega)L/2]\cos[\Delta k(\omega_p, \omega)L] + 1}{\Delta k^2(\omega_p, \omega) + [\alpha(\omega)/2]^2}, \quad (8)$$

where I_p and P_s are the pump intensity and power at the corresponding frequencies on the input face of a nonlinear crystal; P_{THz} is the terahertz radiation power on the output face of the crystal; ε_{vac} is the permittivity of vacuum; $d(\omega)$ is the effective nonlinear coefficient; L is the nonlinear crystal length; and

$$\Delta k(\omega_p, \omega) = k_p(\omega_p) - k_s(\omega_p - \omega) - k(\omega). \quad (9)$$

The frequency dependence $d(\omega)$ for crystals with one phonon resonance in our case can be written in the form [21]

$$d(\omega) = d_e + \frac{d_Q \omega_0^2}{\omega_0^2 - \omega^2 - i\omega\Gamma} = d_e \left(1 + \frac{C\omega_0^2}{\omega_0^2 - \omega^2 - i\omega\Gamma}\right)$$

$$\approx d_e \left(1 + \frac{C\omega_0^2}{\omega_0^2 - \omega^2}\right) = \frac{d(0)}{1 + C}\left(1 + \frac{C\omega_0^2}{\omega_0^2 - \omega^2}\right), \quad (10)$$

where $C = d_Q/d_e$ is the Faust–Henry constant [21] equal to the ratio of the lattice contribution d_Q to the quadratic nonlinear susceptibility to the electron contribution d_e; d_e can be treated approximately as a nonlinear constant responsible for the second harmonic generation in the transparency region of the crystal. One can see from (10) that the nonlinear coefficient $d(\omega)$ vanishes at frequency

$$\omega_{min} = \omega_0 (1 + C)^{1/2}, \quad (11)$$

which is caused by the mutual compensation (destructive interference) of the electron and lattice contributions to the nonlinear susceptibility. This effect is similar to the vanishing of the permittivity $\varepsilon(\omega)$ at the frequencies of longitudinal optical phonons. The Faust–Henry constant can be both positive and negative. It is usually determined by measuring the ratio of the efficiencies of spontaneous Raman scattering of light by longitudinal and transverse optical phonons [13, 21, 22] or, which is more reliable, directly from the frequency dependences of the intensity of Raman scattering by polaritons (for example, by measuring the frequency ω_{min} at which a dip in the Raman scattering intensity is observed) [13]. It is interesting that the constant C for two-atom semiconductor crystals with the symmetry $\bar{4}3m$ is negative, as follows from experiments, and varies from crystal to crystal in the interval approximately from -0.1 to -0.55, i.e. ω_{min} falls within the region of the lower dispersion polariton branch. The Faust–Henry constants and values of ω_{min} calculated from (11) are presented in Table 1.

Note that expressions (3) and (10) determining the dispersions of polaritons and nonlinear susceptibility adequately describe the experimental data obtained for crystals under study. However, the frequency dependence of the polariton absorption $\alpha(\omega)$ calculated by (4) very often differs noticeably from measurements. This is caused by the anharmonicity effects which were neglected in the model used to derive expression (4). The anharmonicity effects are manifested in IR and Raman spectra in the form of additional, usually rather broad bands (resonances) corresponding to the critical Van Hove points in the density distribution of two-phonon states [23]. In the intersection region of the dispersion branches of polaritons with the IR

Table 1. Crystal parameters required for description of the dispersion of polaritons and quadratic nonlinear susceptibility.

Crystal	E_g/eV	ν_0/cm^{-1}	f_0/THz	ν_L/cm^{-1}	f_L/THz	ε_0	ε_∞	References	λ_{cr}/μm	C	ν_{min}/cm^{-1}	f_{min}/THz
GaP	2.34	367	11.00	403	12.11	11.15	9.20	[4]	1.001	−0.48 [14]	265	7.95
CdTe	1.61	143.7	4.31	170	5.10	10.27	7.32	[15]	1.044	−0.10 [16]	136	4.09
ZnTe	2.39	177.5	5.32	207	6.25	9.92	7.18	[15]	0.847	−0.07 [17]	170.7	5.10
GaAs	1.52	269	8.06	292	8.75	12.63	10.72	[18]	1.537	−0.49 [18]	192	5.76

Note: $f_{0,L}(\nu_{0,L})$ are frequencies of the transverse and longitudinal phonons, respectively; $f_{min} = \omega_{min}/2\pi$; $\nu_{min} = \omega_{min}/(2\pi c)$.

regions of two-phonon states, these states interact with each other (polariton Fermi resonance [13, 24]), resulting in the perturbation of the polariton dispersion law and a stronger decay of polaritons due to their additional resonance decomposition into phonon pairs. In most cases, the perturbation of the polariton dispersion branches caused by the Fermi resonance is rather weak [if the bound two-phonon states (biphonons) are not formed in the second-order phonon spectrum], whereas polariton absorption in this region considerably changes (this absorption can differ by several times from that calculated in the quasi-harmonic approximation, and even by an order of magnitude in some cases). In this connection we analysed $\eta(\omega)$ by using polariton absorption spectra experimentally measured in the terahertz frequency range instead of (4).

By selecting cofactors depending on the terahertz frequency ω and assuming that $n(\omega_s) \approx n(\omega_p)$, we can rewrite expression (8), taking into account (3) and (10), in the form

$$\eta(\omega) \equiv \frac{P_{THz}}{P_s} = \frac{2I_p}{\varepsilon_{vac}c^3}\frac{|d(0)|^2}{n^2(\omega_p)n(0)}\omega^2 D(\omega)F_\alpha(\omega_p,\omega)$$

$$= \frac{2I_p}{\varepsilon_{vac}c^3}\frac{|d(0)|^2}{n^2(\omega_p)n(0)}T_\alpha(\omega_p,\omega), \qquad (12)$$

where

$$T_\alpha(\omega_p,\omega) = \omega^2 D(\omega)F_\alpha(\omega_p,\omega); \qquad (13)$$

$$D(\omega) = \left[\frac{d(\omega)}{d(0)}\right]^2\frac{n(0)}{n(\omega)}$$

$$= \frac{\omega_L}{\omega_0}\left[\frac{(1+C)\omega_0^2-\omega^2}{(1+C)(\omega_0^2-\omega^2)}\right]^2\left(\frac{\omega_0^2-\omega}{\omega_L^2-\omega^2}\right)^{1/2}; \qquad (14)$$

$$F_\alpha(\omega_p,\omega) =$$

$$= \frac{\exp[-\alpha(\omega)L]-2\exp[-\alpha(\omega)L/2]\cos[\Delta k(\omega_p,\omega)L]+1}{\Delta k^2(\omega_p,\omega)+[\alpha(\omega)/2]^2}. \qquad (15)$$

Therefore, the frequency dependence of the efficiency of difference frequency generation is described by the function $T_\alpha(\omega_p,\omega)$, which is determined by the product of three factors. The factor ω^2 describes the frequency dependence of the conversion efficiency of nonlinear polarisation to radiation, $D(\omega)$ is determined by the dispersion of quadratic nonlinear susceptibility (10) and dispersion of the refractive index (3) of the crystal in the low-frequency spectral region. The dependences $D(\omega)$ calculated for crystals under study are presented in Fig. 3. The function $F_\alpha(\omega_p,\omega)$ describes the spectral phase matching curve and in the case of weak absorption of a polariton wave [$\alpha(\omega)L \ll 1$], it has the form

$$F_\alpha(\omega_p,\omega) = F_0(\omega_p,\omega) = L^2\mathrm{sinc}^2\left[\frac{\Delta k(\omega_p,\omega)L}{2}\right], \qquad (16)$$

and in the strong absorption limit [$\alpha(\omega)L \gg 1$], it has the form

$$F_\alpha(\omega_p,\omega) = F_\infty(\omega_p,\omega) = \frac{1}{\Delta k^2(\omega_p,\omega)+[\alpha(\omega)/2]^2}. \qquad (17)$$

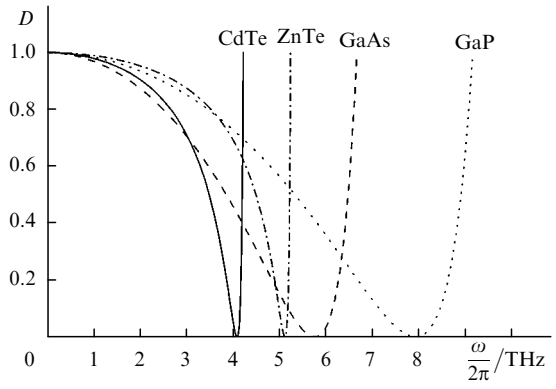

Figure 3. Functions $D(\omega)$ (14) calculated for different crystals.

Consider the physical picture of formation of the spectral distribution of the efficiency of terahertz radiation generation by the example of a CdTe crystal. Figure 4 presents the calculated spectral phase matching curves $F_0(\lambda_p,\omega)$, spectral distributions $T_0(\lambda_p,\omega)$ calculated by neglecting decay and normalised to unity at the maximum, and also spectral distributions $T_\alpha(\lambda_p,\omega)$ calculated taking into account the experimental absorption spectrum of the crystal in the terahertz range obtained in [15]. The calculations were performed for three pump wavelengths $\lambda_p = \lambda_{cr} = 1.044$ μm, $\lambda_p = 1.025$ and 1.0 μm and for three lengths of the nonlinear crystal $L = 1$, 0.5, and 0.25 cm.

For $\lambda_p = \lambda_{cr} = 1.044$ μm, the function $F_0(\lambda_p,\omega)$ (dashed curves in Fig. 4) has one main maximum at the zero frequency with a comparatively large spectral width [because in this case, the function $q(\lambda_p,\omega)$ coincides with the asymptote of the dispersion curve of polaritons for $\omega \to 0$ (Fig. 1)], which increases with decreasing the crystal length. The envelope $T_0(\lambda_p,\omega)$ is mainly determined by the product $\omega^2 F_0(\lambda_p,\omega)$ because $D(\omega)$ very weakly depends on frequency in the region under study (Fig. 3). Due to the presence of the cofactor ω^2, the main maximum of the function $T_0(\lambda_p,\omega)$ [unlike the function $F_0(\lambda_p,\omega)$] is located at a nonzero frequency and shifts to the blue [following the broadening of the main maximum of the function $F_0(\lambda_p,\omega)$] with decreasing the crystal length. The presence of ω^2 also results in the increase in the intensity of side maxima of the function $F_0(\lambda_p,\omega)$. The consideration of absorption (solid curves) leads in this case to a small broadening and red shift of the spectral distribution $T_\alpha(\lambda_p,\omega)$ and the smoothing of side maxima.

For $\lambda_p = 1.025$ μm, the phase matching condition is fulfilled both at the zero frequency and frequency equal approximately to 1.1 THz. The presence of the two maxima is a specific feature of collinear interaction in cubic crystals and considerably affects the spectral distribution of the efficiency of terahertz radiation generation in the low-frequency spectral region. For a large crystal length ($L = 1$ cm), the main maxima of the function $F_0(\lambda_p,\omega)$ are separated by a rather deep dip, which decreases with decreasing the crystal length (dashed curves). This leads to the asymmetry and broadening of the resulting contours (dotted curves), which is most strongly manifested when absorption in a long crystal is taken into account (solid curves) and is caused by strong absorption of terahertz radiation in the vicinity of the maximum. For example, $\alpha \approx 1$ cm^{-1} for $\omega = 1$ THz and $\alpha \approx 10$ cm^{-1} for $\omega = 1.5$ THz, and because of this, the high-frequency tail of the

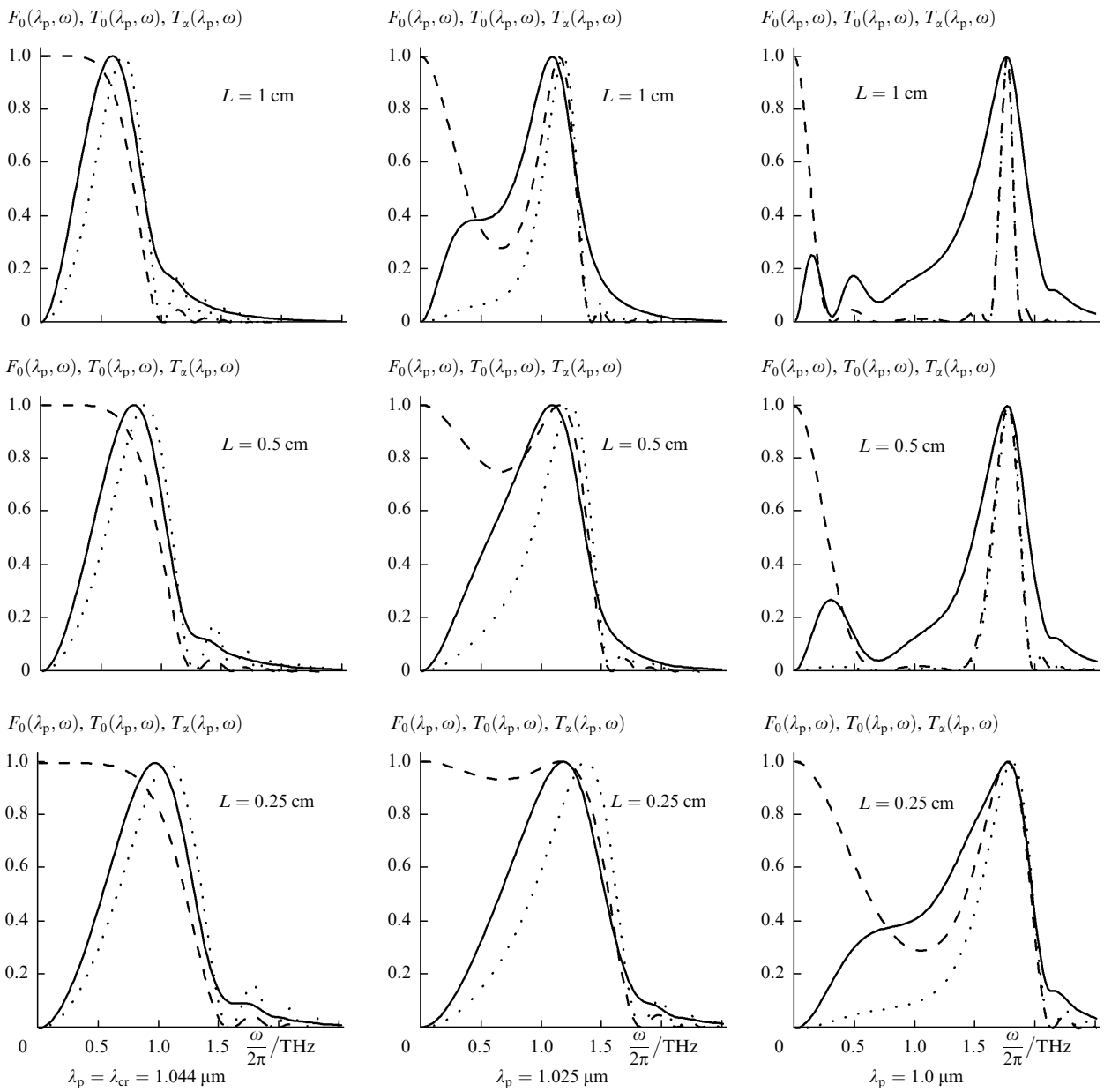

Figure 4. Functions $F_0(\lambda_p,\omega)$ (dashed curves), $T_0(\lambda_p,\omega)$ (dotted curves), and $T_\alpha(\lambda_p,\omega)$ (solid curves) normalised to unity, calculated for a CdTe crystal of different lengths L at different pump wavelengths λ_p.

contour almost does not 'rise' with increasing the crystal length, while the low-frequency tail increases almost proportionally to L^2.

At a lower pump wavelength ($\lambda_p = 1.0$ μm), the second main maximum of the phase matching curves (dashed curves) is shifted to the blue (in accordance with the dispersion phase matching curves presented in Fig. 2), and side maxima is observed between the main maxima in the long crystal. In addition, one can see, by comparing the dotted and solid curves, that the main maximum calculated by neglecting decay is much narrower than that calculated taking the decay into account. This is caused by the influence of absorption on the spectral width of phase matching, which no longer depends on the crystal length and is determined by absorption [$F_0(\lambda_p,\omega) \to F_\infty(\lambda_p,\omega)$].

Thus, the spectra presented in Fig. 4 illustrate the formation of the spectral distribution of the efficiency of terahertz radiation generation and its dependence on the pump wavelength, absorption, and length of a nonlinear optical crystal. One can see that the spectral distribution can be controlled by varying both the pump wavelength and the crystal length.

As a whole, the general picture is also preserved for other crystals. The spectral distributions $T_\alpha(\lambda_p,\omega)$ calculated for different crystals as functions of λ_p and L taking absorption into account are demonstrated in Fig. 5. The function $T_\alpha(\lambda_p,\omega)$ is presented in absolute units with the dimensionality $\mathrm{THz}^2\,\mathrm{cm}^2$, which allows us to compare frequency factors for different crystals. We used in calculations the experimental absorption spectra in the terahertz range taken from [15] for CdTe and ZnTe crystals and from [25] for GaP and GaAs crystals.

Expression (12) can be written in the form

$$\eta(\omega) = 3.3 \times 10^{-13}\,\mathrm{FOM}\, I_p T_\alpha(\lambda_p,\omega), \qquad (18)$$

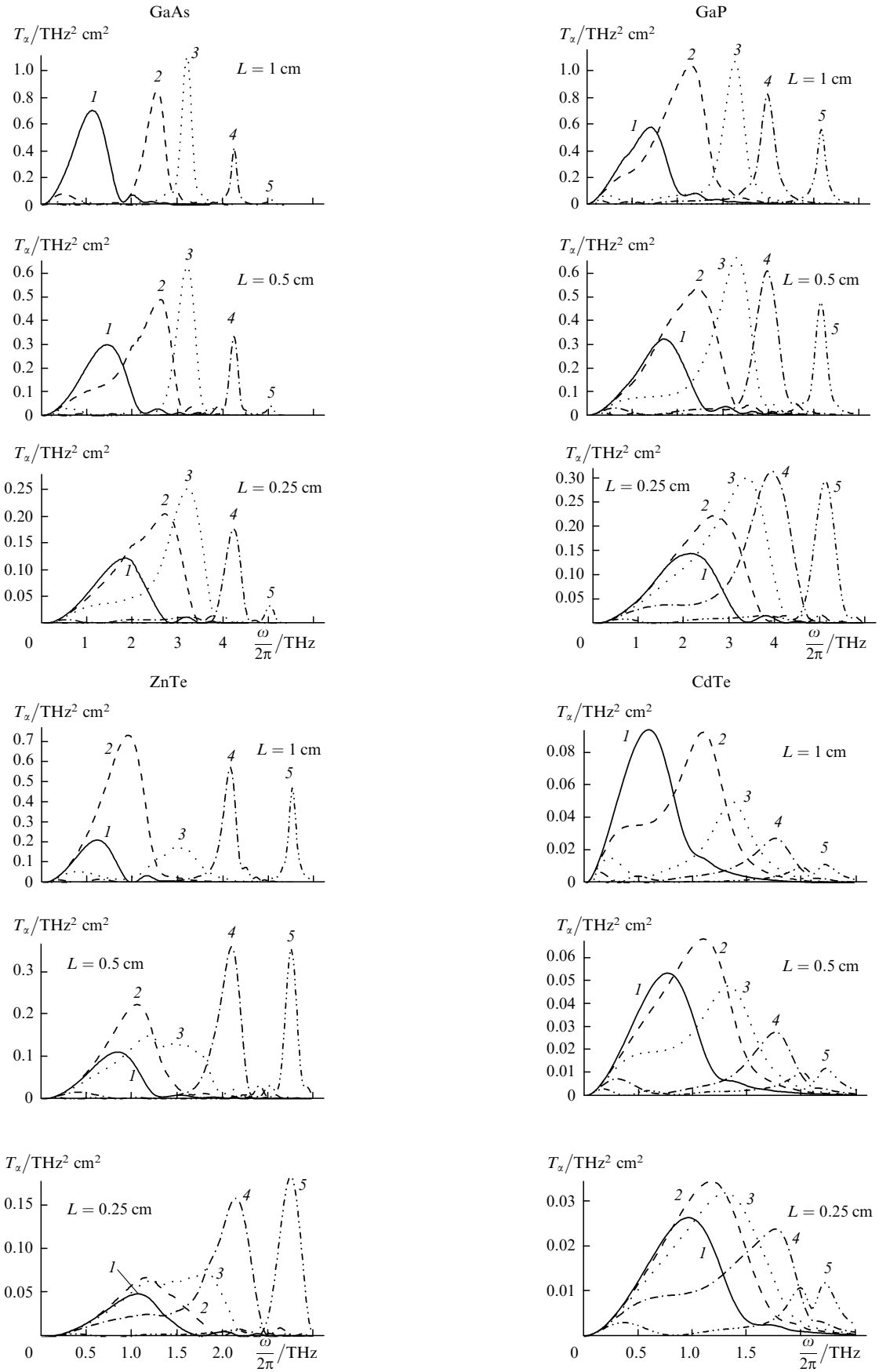

Figure 5. Spectral distributions of the efficiency $T_\alpha(\lambda_p, \omega)$ (13) of difference frequency generation in the terahertz region calculated for four crystals of difference length L at pump wavelengths 1.5373 (*1*), 1.45 (*2*), 1.4 (*3*), 1.3 (*4*), and 1.2 μm (*5*) for GaAs; 1.001 (*1*), 0.98 (*2*), 0.96 (*3*), 0.94 (*4*), and 0.9 μm (*5*) for GaP; 0.8467 (*1*), 0.83 (*2*), 0.81 (*3*), 0.79 (*4*), and 0.75 μm (*5*) for ZnTe; 1.044 (*1*), 1.025 (*2*), 1.015 (*3*), 1.0 (*4*), and 0.977 μm (*5*) for CdTe.

which is convenient for comparing and optimisation of the conditions of terahertz radiation generation in different crystals. Here, I_p is expressed in W cm^{-2}, $T_\alpha(\lambda_p, \omega)$ in THz^2 cm^2, and FOM (figure of merit) in pm^2 V^{-2}. The FOM is the frequency-independent figure of merit of a nonlinear crystal for generation of terahertz radiation (excitation of polaritons of the lower dispersion branch):

$$\mathrm{FOM} = \frac{|d(0)|^2}{n^2(\omega_{cr})n(0)}. \quad (19)$$

The value of $d(0)$ can be determined from the experimental value of the constant r of linear electrooptical effect (for a 'clamped' crystal), which is related to $d(0)$ by the expression [22]

$$d(0) = -\frac{n^4(\omega_{cr})r}{4}. \quad (20)$$

The FOM values found in this way are presented in Table 2. Constants r were taken from [19]. Figure 5 presents functions $T_\alpha(\lambda_p, \omega)$ obtained for crystals under study.

Table 2. Crystal parameters required for calculations of the efficiency of terahertz radiation generation.

Crystal	r/pm V^{-1}	$n(\lambda_{cr})$	$d(0)$/pm V^{-1}	FOM $= \frac{n^6(\lambda_{cr})r^2}{16n(0)}$/pm^2 V^{-2}
GaP	1.0	3.12	24	17
CdTe	4.5	2.79	68	186
ZnTe	4.3	2.83	69	189
GaAs	1.5	3.38	49	71

4. Conclusions

We have established the general properties of the spectral distribution of the efficiency of terahertz radiation generation in zinc blende semiconductor crystals, where the difference frequency upon collinear propagation of interacting waves is tuned by changing the pump wavelength (due to dispersion phase matching). In this propagation scheme, the spectral phase matching curves have two main maxima, which results in a strong broadening, asymmetry, and appearance of an additional structure in the low-frequency region of the spectral distribution of the efficiency of terahertz radiation generation. It has been shown that the spectral distribution can be controlled by changing both the pump wavelength and the length of a nonlinear optical crystal.

References

1. Shen Y.R. *Prog. Quantum Electron.*, **4**, 207 (1978).
2. Mittleman D. (Ed.) *Sensing with Therahertz Radiation* (Springer Series in Optical Sciences, Vol. 85; Berlin: Springer, 2003); *Dig. of 2004 Joint XXIX Int. Conf. on Infrared and Millimeter Waves and XII Int. Conf. on Teraherts Electronics* (Karskuhe, Germany, University of Karlsruhe, 2004).
3. Kawase K., Shikata J., Ito H. *J. Phys. D*, **35**, R1 (2002).
4. Tanabe T., Suto K., Nishizawa J., Saito K., Kimura T. *J. Phys. D*, **36**, 953 (2003).
5. Shi W., Ding Y.J., Fernelius N., Vodopyanov K. *Opt. Lett.*, **27**, 1454 (2002).
6. Shi W., Ding Y.J. *Opt. Lett.*, **30**, 1030 (2005).
7. Tochitsky S.Ya., Ralph J.E., Sung C., Joshi C. *J. Appl. Phys.*, **98**, 026101 (2005).
8. Xu L., Zhang A.G., Auston D.H. *Appl. Phys. Lett.*, **61**, 784 (1992).
9. Nahata A., Weling A.S., Heinz T.F. *Appl. Phys. Lett.*, **69**, 2321 (1996).
10. Ahn J., Efimov A.V., Averitt R.D., Taylor A.J. *Opt. Express*, **11**, 2486 (2000).
11. Wahlstrand J.K., Merlin R. *Phys. Rev. B*, **68**, 054301 (2003).
12. Hebling J., Stepanov A.G., Almasi G., Bartal B., Kuhl L. *Appl. Phys. B*, **78**, 593 (2004).
13. Polivanov Yu.N. *Usp. Fiz. Nauk*, **126**, 185 (1978).
14. DeMartini F. *Phys. Rev. B*, **4**, 4546 (1971).
15. Schall M., Walther M., Jepsen P.U. *Phys. Rev. B*, **64**, 094301 (2001).
16. Bairamov B.H., Toropov V.V., Agrinskaya N.V., Samedov E.A., Irmer G., Monecke J. *Phys. Stat. Sol. (b)*, **146**, K161 (1988).
17. Leitenstorfer A., Hunsche S., Shah J., Nuss M.C., Knox W.H. *Appl. Phys. Lett.*, **74**, 1516 (1999).
18. Nippus M., Claus R. *Zs. Natürf.*, **32a**, 731 (1977).
19. Kikoin I.K. (Ed.) *Tablitsy fizicheskikh velichin* (Tables of Physical Quantities) (Moscow: Atomizdat, 1976).
20. Yang K.H., Morris J.R., Richards P.L., Shen Y.R. *Appl. Phys. Lett.*, **23**, 669 (1973).
21. Faust W.L., Henry C.H. *Phys. Rev. Lett.*, **17**, 1265 (1966).
22. Johnston W.D. Jr, Kaminov I.P. *Phys. Rev.*, **188**, 1209 (1969).
23. Poulet H., Mathieu J.P. *Vibrational Spectra and Symmetry of Crystals* (Paris: Gordon and Breach, 1970; Moscow: Mir, 1973).
24. Agranovich V.M., Lalov I.I. *Usp. Fiz. Nauk*, **146**, 267 (1985).
25. Palik E.D. *Handbook of Optica Constants of Solids* (New York: Acad. Press, 1998) Vol. III.